Journal of Modern Optics
Vol. 00, No. 00, DD Month 200x, 1–15

Classical aspects of laser-induced nonsequential double ionisation above and below the threshold

C. Figueira de Morisson Faria
Centre for Mathematical Science, City University, Northampton Square, London EC1V OHB, United Kingdom
X.Liu
Department of Physics, Texas A&M University, College Station, TX 77843-4242, USA
W. Becker
Max-Born-Institut, Max-Born-Str. 2a, 12489 Berlin, Germany
(Received 00 Month 200x; In final form 00 Month 200x)

The S-matrix element for nonsequential double ionisation of an atom irradiated by a high-intensity near-infrared laser field via the recollision–impact-ionisation scenario is investigated with particular emphasis on a certain classical limit where classical kinematics govern throughout and wave-packet spreading is ignored. The resulting classical model is applied to the calculation of the one-electron energy spectrum in coincidence with double ionisation. Various assumptions are made for the interaction by which the returning electron frees the second, up to this time inactive, electron and its initial wave function. The resulting momentum correlations of the two emitted electrons are investigated just above and below the threshold intensity, for which the maximal energy of the recolliding electron equals the ionisation energy of the singly-charged ion, and the quantum-mechanical amplitude and the classical approximation are compared. The classical model is extended to intensities below this threshold by making allowance for the escape threshold being lowered by the laser field.

1 Introduction

One-photon double ionisation of an atom is almost a paradigm of a many-particle process that requires both quantum mechanics and electron-electron correlation for its existence. In contrast, nonsequential *multiphoton* double ionisation (NSDI) by a high-intensity infrared field (for a review of NSDI, see reference [1]; for a comparison of single-photon and multiphoton double ionisation, see [2]) is much closer to the classical domain, so close actually that the question has been raised whether it requires quantum mechanics at all [3]. In this paper, we will not adopt such a radical point of view. Rather, we will stay within the by now well established scenario wherein NSDI gets started by one electron tunneling quantum mechanically into the continuum. Whatever happens thereafter is treated classically. Indeed, within the past few years, just

about any aspect of NSDI has been investigated and described within such a partly classical framework, generally with good success. This includes the role of electron-impact ionisation vs. electron-impact excitation [4], the significance of Coulomb refocusing [5], the distribution of the momentum of the doubly charged ion [6], energy-resolved angular distributions of the photoelectrons in coincidence with double ionisation [7], the correlation of the longitudinal-momentum components of the two electrons [8–10], the possible pathways for double and multiple ionisation [11, 12], the role of different types of collisions leading to NSDI [13] and, more recently, NSDI with few-cycle laser pulses [14, 15].

In this paper, we will be specifically concerned with a certain classical limit of the standard rescattering–impact-ionisation S-matrix element that has been investigated and computed by several groups [9, 10, 15–18]. This S-matrix element incorporates in a coherent fashion tunneling of the most loosely bound electron into the continuum, its subsequent acceleration by the laser field followed by recollision with its parent ion and inelastic scattering whereby the second electron is set free. The final momentum distribution of the two electrons is to a great extent determined by the laser field, which further accelerates the two electrons after the inelastic rescattering event. In particular, in previous publications, we have computed differential electron momentum distributions employing saddle-point methods within this S-matrix framework [9,10,15,16]. The classical limit of this S-matrix element suppresses quantum-mechanical wave-packet spreading during the propagation of the electron in its intermediate state. This leads to a very simple approximation, which has been shown to yield excellent agreement with the fully quantum-mechanical S-matrix element for high intensities [9,10,15,16]. Here, we will employ this classical limit to calculate the electron energy spectrum in coincidence with NSDI, when only one electron is observed, as has been done in a series of high-precision experiments [19–23].

The classical limit becomes inapplicable when the laser intensity reaches the point that the kinetic energy of the returning electron no longer suffices to release the second electron. For intensities just above and below this limit, we will study the electron-electron correlation using different wave functions for the initial state of the second bound electron as well as different forms of the interaction by which the returning first electron interacts with the second. The minimal energy that the bound electron requires to escape is lower than its field-free value due to the presence of the laser field [24]. Recent experiments have invoked this fact in order to explain the observation that the shape of the momentum-momentum correlation hardly changes when the field intensity is reduced below the afore-mentioned threshold [25]. Here, we incorporate the lowered threshold by hand into the classical model and explore the consequences.

The paper is organized as follows: In section 2, we provide the necessary theoretical background for discussing the results presented in the subsequent sections concentrating, in particular, on the classical limit (section 3). Such results concern one the electron momentum distribution emitted in NSDI (section 4), and nonsequential double ionisation below the threshold (section 5). Finally, we summarize the paper with some concluding remarks (section 6).

2 Theory

The quantum-mechanical S-matrix element for nonsequential double ionisation from an initial two-electron bound state $|\psi_0(t')\rangle$ with binding energies E_{01} and E_{02} of the two electrons into a final continuum state $|\psi_{\mathbf{p}_1\mathbf{p}_2}\rangle$ with asymptotic momenta $\mathbf{p}_1$ and $\mathbf{p}_2$ is

$$M = -\int_{-\infty}^{\infty} dt \int_{-\infty}^{t} dt' \langle \psi_{\mathbf{p}_1\mathbf{p}_2}(t)|V_{12}U_1^{(\mathrm{V})}(t,t')V_1U_2^{(0)}(t,t')|\psi_0(t')\rangle. \quad (1)$$

This matrix element formalizes the rescattering–impact-ionisation scenario described above. The quantities V_1 and $U_1^{(\mathrm{V})}(t,t')$ denote the atomic binding potential and the Volkov time-evolution operator acting on the first electron, $U_2^{(0)}(t,t')$ is the field-free propagator acting on the second electron for as long as it it is bound, and V_{12} is the electron-electron interaction through which the second electron is freed by the recolliding first. A rather compact evaluation becomes feasible once we approximate the initial bound state by a product state,

$$|\psi_0(t)\rangle = |\psi_0^{(1)}(t)\rangle \otimes |\psi_0^{(2)}(t)\rangle, \quad (2)$$

and the final state by a Volkov state, which may or may not take the electron-electron Coulomb repulsion into account [10, 15].

The matrix element (1) exhibits two temporal integrations over the times t and t' where $t > t'$. In a semiclassical interpretation, t' is the time when the first electron tunnels into the continuum to begin its orbit with velocity $\mathbf{v}(t') = 0$. The time t when the first electron revisits the ion in order to rescatter then is a (multivalued) function of t', $t \equiv t(t')$, which is readily determined numerically from the classical equations of motion. Quantum mechanically, t and t' are independent, since the electron is not exactly confined to its classical orbit and the initial velocity is not necessarily zero. However, the dominant contributions to the integral come from times that are related by the above condition $t = t(t')$. Furthermore, such contributions can be traced back to the orbits of a classical electron in an external laser field.

The above statement can be explicitly shown as follows. If $U_1^{(\mathrm{V})}(t,t')$ is expanded into Volkov states, equation (1) reads

$$M = -\int_{-\infty}^{\infty} dt \int_{-\infty}^{t} dt' \int d^3k V_{\mathbf{p_n},\mathbf{k}} V_{\mathbf{k},0} \exp[iS(t,t',\mathbf{p}_n,\mathbf{k})], \tag{3}$$

with the action

$$\begin{aligned} S(t,t',\mathbf{p}_n,\mathbf{k}) = &-\frac{1}{2}\sum_{n=1}^{2}\int_{t}^{\infty}[\mathbf{p}_n + \mathbf{A}(\tau)]^2 d\tau \\ &-\frac{1}{2}\int_{t'}^{t}[\mathbf{k} + \mathbf{A}(\tau)]^2 d\tau + |E_{01}|t' + |E_{02}|t, \end{aligned} \tag{4}$$

where $\mathbf{A}(t)$, $\mathbf{p}_n$, $\mathbf{k}$, and $|E_{0n}|$ $(n = 1,2)$ denote the vector potential, the final momenta, the intermediate momentum, and the ionisation potentials, respectively. The binding potential V and the electron-electron interaction V_{12} have been absorbed into the form factors

$$V_{\mathbf{p}_n,\mathbf{k}} = \langle \mathbf{p}_2 + \mathbf{A}(t), \mathbf{p}_1 + \mathbf{A}(t) | V_{12} | \mathbf{k} + \mathbf{A}(t), \psi_0^{(2)} \rangle \tag{5}$$

and

$$V_{\mathbf{k},0} = \langle \mathbf{k} + \mathbf{A}(t') | V | \psi_0^{(1)} \rangle. \tag{6}$$

The detailed shape of the distributions of the final momenta is governed by the form factor $V_{\mathbf{p}_n,\mathbf{k}}$, which is essentially the Fourier transform of the electron-electron interaction, with the bound state $|\psi_0^{(2)}\rangle$ of the initially inactive electron in place of a plane wave.

We compute the five-dimensional integral in the transition amplitude (3) employing a uniform saddle-point approximation, whose only applicability requirement is that the saddles occur in pairs. This is the case in rescattering problems ocurring within the context of intense laser-atom physics [26]. The equations that determine the saddle points, obtained from the condition that $S(t,t',\mathbf{p}_n,\mathbf{k})$ $(n = 1,2)$ be stationary, can be directly related to the classical equations of motion of an electron in an external laser field. This shows that the dominant contributions to the quantum-mechanical amplitude correspond to the classical paths of an electron rescattering off its parent ion, as stated above. These saddle-point equations read

$$\left[\mathbf{k} + \mathbf{A}(t')\right]^2 = -2|E_{01}| \tag{7}$$

$$\sum_{n=1}^{2}[\mathbf{p}_n+\mathbf{A}(t)]^2=[\mathbf{k}+\mathbf{A}(t)]^2-2|E_{02}| \tag{8}$$

$$\int_{t'}^{t}d\tau\,[\mathbf{k}+\mathbf{A}(\tau)]=0. \tag{9}$$

They correspond to energy conservation at the time the first electron tunnels out, to energy conservation upon rescattering, and to the condition that the first electron return to the site of its release, respectively. In the limit $|E_{01}|\rightarrow 0$, the classical case is recovered. In terms of the momentum components parallel and perpendicular to the laser field polarisation, equation (8) reads

$$\sum_{n=1}^{2}\left[p_{n||}+A(t)\right]^2+\sum_{n=1}^{2}\mathbf{p}_{n\perp}^2=[\mathbf{k}+\mathbf{A}(t)]^2-2|E_{02}|, \tag{10}$$

which describes a hypersphere in the six-dimensional $(p_{n\parallel},\mathbf{p}_{n\perp})$ space, whose radius depends on t. The union of all these hypersphere for all t determines the region in momentum space for which electron-impact ionisation is allowed to occur within a classical framework. For momenta outside this region, we will refer to this process as "classically forbidden". Hence, if all radii have collapsed to zero, electron-impact ionisation will be forbidden throughout. Concrete examples of such a situation are given in [14,15], in case the driving field is a few-cycle pulse, and in section 5 of this paper, for nonsequential double ionisation below the threshold. More details about the saddle-point methods used in this paper are given in [10].

3 The classical limit

With all this in mind, we write down the classical limit of the quantum-mechanical yield $|M|^2$ as

$$F(\mathbf{p}_1,\mathbf{p}_2)=\int dt' R(t')\delta\left(\frac{1}{2}[\mathbf{p}_1+\mathbf{A}(t)]^2 +\frac{1}{2}[\mathbf{p}_2+\mathbf{A}(t)]^2+|E_{02}|-E_{\rm ret}(t)\right)|V_{\mathbf{pk}(t)}|^2. \tag{11}$$

There is one integral over the ionisation time t' when the first electron appears in the continuum at the time-dependent rate $R(t')\equiv R(E(t'))$, for which we may take the standard expression $R(t')\sim |E(t')|^{-1}\exp\left[-2(2|E_{01}|)^{3/2}/(3|E(t')|)\right]$ [27]. The δ function describes energy

conservation in the inelastic rescattering process at the rescattering time $t = t(t')$ when the electron returns to the ion with momentum $\mathbf{k}(t)$ and kinetic energy $E_{\rm ret} \equiv (1/2)\mathbf{k}^2(t) = (1/2)[\mathbf{A}(t) - \mathbf{A}(t')]^2$.

The following quantum features have been eliminated in going from the S-matrix element (1) to the classical yield (11). First, in the classical model there is no spreading of the electronic wave packet from the ionisation time t' to the return time t. Second, for given $\mathbf{p}_1$ and $\mathbf{p}_2$, as remarked above, there are several solutions $t \equiv t(t')$. In quantum mechanics, their contributions are added coherently in the *amplitude*, while in the classical yield (11) the *probabilities* corresponding to the various solutions are added. Further, below the classical threshold the argument of the δ function in equation (11) is nonzero for any ionisation time t' so that the yield is zero. Quantum mechanics admits a larger energy transfer from the laser field to the charged particles, so that the yield remains nonzero, though it becomes exponentially small when the parameters move into the nonclassical regime. This implies that the classical model becomes already unreliable near the boundaries of the classical region. Finally, in quantum mechanics there is no well-defined instant when the electron is "born" and, therefore no zero initial velocity at this time.

If the second electron is dislodged by a contact-type interaction placed at the origin, the form factor $V_{\mathbf{p}_n\mathbf{k}(t)}$ is constant, i.e., independent of the final momenta as well as the momentum of the returning electron. It is then a very easy matter to carry out integrations over subsets of the final-momentum components. To this end, we introduce in equation (11) the Fourier transform of the δ function,

$$\delta(x) = \int_{-\infty}^{\infty} \frac{d\lambda}{2\pi} \exp(-i\lambda x).$$

Finite or infinite integrations over momentum components $\mathbf{p}_n$ in Eq. (11) then reduce to Gaussian integrals. In the end, the remaining integration over λ is done with the help of [28]

$$\int_{-\infty}^{\infty} \frac{d\lambda}{(i\lambda+\epsilon)^\nu} e^{ip\lambda} = \frac{2\pi}{\Gamma(\nu)} p_+^{\nu-1}, \tag{12}$$

where $x_+^\nu = x^\nu\theta(x)$, with $\theta(x)$ the unit step function and $\epsilon \to +0$.

Here, we will consider two examples. In section 5, we will be interested in the distribution of the momentum components parallel to the laser field regardless of the transverse components $\mathbf{p}_\perp$, for which we obtain

$$\int d^2\mathbf{p}_{1\perp} d^2\mathbf{p}_{2\perp} F(\mathbf{p}_1, \mathbf{p}_2) = 4\pi^2 \int dt' R(t') (\Delta E)_+ \tag{13}$$

with

$$\Delta E \equiv \Delta E(p_{1\parallel}, p_{2\parallel}, t) \equiv E_{\rm ret}(t) - |E_{02}| - \frac{1}{2}[p_{1\parallel} + A(t)]^2 - \frac{1}{2}[p_{2\parallel} + A(t)]^2. \quad (14)$$

Sufficiently far above the threshold, the distribution (13) agrees very well with the corresponding distribution computed from the fully quantum-mechanical amplitude (1) [9, 10]. Remarkably, it also agrees quite well with the corresponding experimental measurements in the case of neon, where rescattering–impact-ionisation appears to be the dominant NSDI mechanism [29].

Second, in the following section, we will consider the (three-dimensional) momentum distribution of one electron in nonsequential double ionisation, regardless of the momentum (parallel plus transverse) of the other. This is

$$\int d^3\mathbf{p}_2 F(\mathbf{p}_1, \mathbf{p}_2) = 4\pi\sqrt{2} \int dt' R(t') \left(\Delta E_1\right)_+^{1/2} \quad (15)$$

with $\Delta E_1 \equiv E_{\rm ret}(t) - |E_{02}| - \frac{1}{2}[\mathbf{p}_1 - e\mathbf{A}(t)]^2$. Other distributions, including those resulting from nonsequential multiple ionisation, can be evaluated with comparable ease.

4 One-electron kinetic energy spectra

One-electron momentum spectra correlated with double ionisation have been recorded in several experiments [19–23]. Compared with the electron spectra emitted in single ionisation, the data (when plotted versus energy in multiples of the ponderomotive energy U_p) show a preponderance of hot electrons with energies exceeding $2U_p$ and a less pronounced dependence on the atomic species [22]. Here we present a detailed comparison of the results of our model presented in the preceding section and expressed in equation (15) with the data of Chaloupka et al. [22]. The electron energy spectra were registered in coincidence with a doubly charged ion for all rare gases, and detected along the laser polarisation direction within a solid angle of about 10°, regardless of the momentum (parallel and transverse) of the second electron. In figure 1, we plot the quantity

$$\frac{dN}{\sqrt{2E}dEd\Omega} \sim \int d^3\mathbf{p}_2 F(\mathbf{p}_1, \mathbf{p}_2) \quad (16)$$

which is computed from equation (15) and where $E = \mathbf{p}_1^2/2$ is the electron energy. Up to the factor of $\sqrt{2E}$, it is proportional to the one-electron energy spectrum for emission into the solid angle $d\Omega$ along the polarisation direction

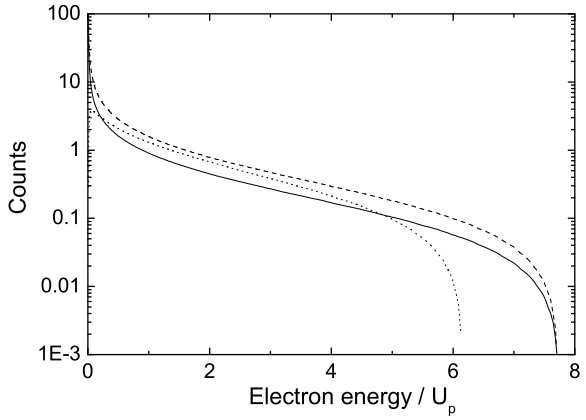

Figure 1. One-electron energy spectra (16) in coincidence with double ionisation of various noble gases. Solid line: He at laser intensity $I = 8 \times 10^{14}\mathrm{W/cm}^2$, dashed line: Ne at $I = 6 \times 10^{14}\mathrm{W/cm}^2$, dotted line: Ar at $I = 2.5 \times 10^{14}\mathrm{W/cm}^2$.

of the laser field in coincidence with NSDI, when the second electron is not observed. We divided by $\sqrt{2E}$ in order to remove the trivial zero at zero energy, which is due to phase space. The results are for helium, neon, and argon, for the parameters of the data of reference [22]. (The data for krypton and xenon in [22] were recorded at laser intensities just above and far below the classical threshold, respectively, so that our classical model does not apply. A discussion of how to extend the classical model to laser intensities below the threshold is given in the next section.)

In the experimental data [22], the measured electron spectrum starts to decrease at a kinetic energy near $4.3U_p$ for He. For all other rare gases, the measured spectra extend beyond $6U_p$, which is the highest electron energy for which data are shown. In our calculations, the electron spectra experience their cutoffs at about $6.2U_p$ for argon and $7.8U_p$ for helium and neon in agreement with the classical cutoff laws derived in reference [30]. These cutoff laws delineate the boundaries of the classically accessible region of phase space. It depends on the dynamics of the process, partly expressed in the form factors (5), whether the classically accessible region is actually populated. A contact interaction generates momentum distributions that take full advantage of the available phase space, while a Coulomb interaction leaves the regions with high momenta largely empty. The fact that the data for helium appear to exhibit a cutoff that is lower than our results may point to the fact that in helium (unlike neon) the effective electron-electron interaction V_{12} is closer to a pure Coulomb potential. Our results reproduce the (on the semilogarithmic scale) approximately linear decrease of the data with about the same slope

for all atomic species. This suggests that our extremely simple classical model provides at least a useful benchmark at laser intensities that are well above the classical threshold. Similar results have been obtained within the fully quantum-mechanical S-matrix theory of Becker and Faisal for helium at the highest laser intensity [31].

5 NSDI below the threshold

In the previous sections, we have shown that simple classical models give a satisfactory description of nonsequential double ionisation, as long as the driving-field intensity is high enough. This, however, is no longer true if the first electron does not return with sufficient energy to release the second electron. In our framework, this means that electron-impact ionisation is forbidden in the whole momentum space. In the literature, this intensity regime is referred to as "below the threshold". While, in this case, the classical yields vanish, quantum mechanically there is still a small probability that the second electron reaches the continuum. Specifically, measurements of NSDI differential electron distributions below the threshold have been recently reported and revealed maxima both along the diagonal $p_{1||} = p_{2||}$ and also (less pronounced and very surprisingly) along the anti-diagonal $p_{1||} = -p_{2||}$, in the plane of the momentum components parallel to the laser-field polarisation [25].

In the following, we investigate differential electron momentum distributions below the threshold. In particular, we address the question of how these distributions are influenced by the type of interaction V_{12}, by which according to equation (1) the second electron is released, as well as by the states in which the electrons are initially bound. For intensities far above the threshold, a similar investigation has been performed in [16]. Therein, we considered that both electrons are bound in s and p states and, additionally, that the second electron is initially localized at $\mathbf{r}_2 = 0$. We found that spatially extended wave functions cause a broadening in the momentum distributions in the direction $p_{1||} = -p_{2||}$, even if V_{12} is of contact type. Indeed, circular-shaped distributions are only obtained if the initial wave function of the second electron exhibits no spatial extension. Formally, this corresponds to restricting the contact-type interaction to the position of the ion (at the origin of the coordinate system), as was done in previous publications [9, 10, 15]. There is, however, a further change in the shapes of the distributions if a Coulomb-type interaction frees the second electron. In this case, such an interaction enhances the yield for unequal momenta. This agrees with former results [18].

In this paper, we will investigate the effect of different initial wave functions solely for the second electron. Different initial states for the first electron only have a minor influence in the region of small parallel momenta, and will not

be considered here[1] (for details, cf. Ref. [16]). We will consider the case that the second electron is initially in a $1s$ state or a $2p$ state or in a bound state extremely strongly localized at $\mathbf{r}_2 = 0$. For a contact-type interaction, such that $V_{12} \sim \delta(\mathbf{r}_1 - \mathbf{r}_2)$, this yields the form factors

$$V^{(1s)}_{\mathbf{p}_n,\mathbf{k}} \sim \frac{1}{[2|E_{02}| + \tilde{\mathbf{p}}^2]^2}, \tag{17}$$

$$V^{(2p)}_{\mathbf{p}_n,\mathbf{k}} \sim \frac{\tilde{p}}{[2|E_{02}| + \tilde{\mathbf{p}}^2]^3}, \tag{18}$$

$$V^{(\delta)}_{\mathbf{p}_n,\mathbf{k}} = \text{const}, \tag{19}$$

respectively, with $\tilde{\mathbf{p}} = \mathbf{p}_1 + \mathbf{p}_2 - \mathbf{k} + \mathbf{A}(t)$. The last case (19) is equivalent with a three-body contact interaction $V_{12} \sim \delta(\mathbf{r}_1 - \mathbf{r}_2)\delta(\mathbf{r}_2)$. If V_{12} is of Coulomb-type, the corresponding form factors are given by

$$V^{(1s)}_{\mathbf{p}_n,\mathbf{k}} \sim \frac{1}{[\mathbf{p}_1 - \mathbf{k}]^2\,[2|E_{02}| + \tilde{\mathbf{p}}^2]^2} + \mathbf{p}_1 \leftrightarrow \mathbf{p}_2. \tag{20}$$

$$V^{(2p)}_{\mathbf{p}_n,\mathbf{k}} \sim \frac{1}{[\mathbf{p}_1 - \mathbf{k}]^2}\,\frac{\tilde{p}}{[2|E_{02}| + \tilde{\mathbf{p}}^2]^3} + \mathbf{p}_1 \leftrightarrow \mathbf{p}_2, \tag{21}$$

$$V^{(\delta)}_{\mathbf{p}_n,\mathbf{k}} \sim \frac{1}{[\mathbf{p}_1 - \mathbf{k}]^2} + \mathbf{p}_1 \leftrightarrow \mathbf{p}_2, \tag{22}$$

respectively.

We estimate the threshold intensity as the intensity for which the radius in equation (8) collapses. In this estimate, we assume that the electron transverse momenta are vanishing. This yields an upper bound for such a radius and, consequently, for the region in the $(p_{1||}, p_{2||})$ plane for which electron-impact ionisation is classically allowed. Such a condition occurs if the kinetic energy $[A(t) - A(t')]^2/2$ of the first electron upon return is equal to the second ionisation potential $|E_{02}|$. Since the maximal kinetic energy of the returning electron is $E^{(\max)}_{\text{ret}} = 3.17U_p$, the threshold intensity corresponds roughly to

[1] In our framework, the initial bound-state wave functions $\varphi^{(2)}_0(\mathbf{r}_2)$ and $\varphi^{(1)}_0(\mathbf{r}_1)$, of the second and first electron, affect the form factors $V_{\mathbf{p}_n\mathbf{k}}$ and $V_{\mathbf{k}0}$, respectively. The form factor $V_{\mathbf{p}_n\mathbf{k}}$ is related to the interaction by which the second electron is dislodged and has a major influence on the shapes of the differential electron momentum distributions, whereas $V_{\mathbf{k}0}$ only slightly affects the potential barrier through which the first electron tunnels out. This has been shown in a previous paper (Ref. [16]), in which we have incorporated the latter form factor in the time-dependent action. This led to modifications in the quantum orbits, which caused only a minor suppression in the region of small parallel momenta, as compared to the case in which $V_{\mathbf{k}0}$ is assumed to be constant.

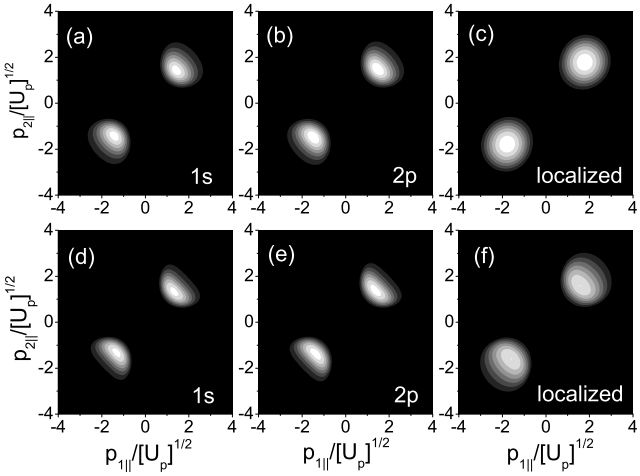

Figure 2. Electron momentum distributions computed using the classical model for neon ($|E_{01}| = 0.79$ a.u. and $|E_{02}| = 1.51$ a.u.) subject to a linearly polarized monochromatic field with frequency $\omega = 0.057$ a.u. and intensity $I = 3.0 \times 10^{14}\mathrm{W/cm}^2$, as functions of the electron momentum components parallel to the laser-field polarisation. The upper and lower panels have been computed for a contact and Coulomb-type interaction V_{12}, respectively. In panels (a) and (d), and (b) and (e), the second electron is taken to be initially in a $1s$, and in a $2p$ state, respectively, whereas in panels (c) and (f) the spatial extension of the bound-state wave function has been neglected. The transverse momenta have been integrated over.

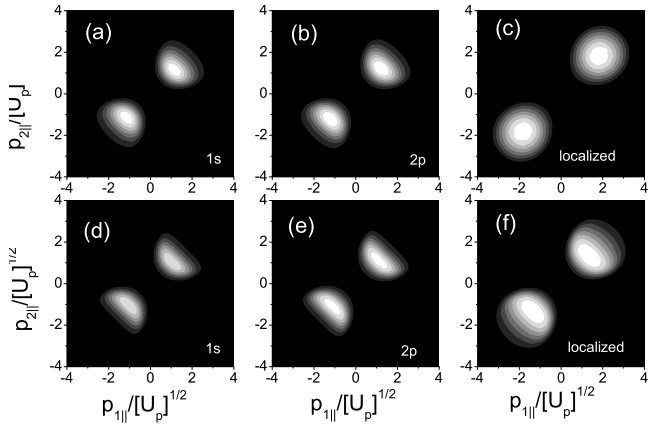

Figure 3. Same as figure 2 but computed using the quantum-mechanical model.

$3.17U_p \sim |E_{02}|$. One should note that, at such an intensity, the Keldysh parameter $\gamma = \sqrt{|E_{01}|/(2U_p)}$ is still smaller than unity, so that the system is in the tunneling regime and the formalism discussed in section 2 is applicable. In fact, the multiphoton regime is reached at the much lower driving-field intensity for which $|E_{01}| = 2U_p$. For neon, which we will consider in the following results, the threshold intensity lies around $I_{\mathrm{t}} \simeq 2.2 \times 10^{14}\mathrm{W/cm}^2$, and the

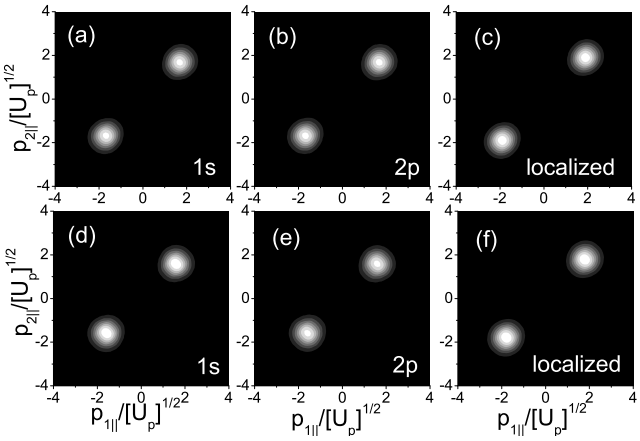

Figure 4. Same as figure 3, but for the lower intensity of 1.8×10^{14} Wcm^{-2}.

tunneling regime extends down to $I_{\min} \simeq 1.8 \times 10^{14}$W/cm^2.

Before we focus on the intensity regime below the threshold, we perform calculations at intensities closely above the classical threshold, to check to which extent the afore-mentioned classical model can still be applied in this regime. In figure 2, we present results obtained slightly above the threshold intensity, computed employing the classical model. Such results are sensitive to the choice of the interaction V_{12} by which the second electron is released, and to the spatial extent of the initial electronic wave function $\varphi^{(2)}(\mathbf{r}_2)$. Indeed, the changes in the shapes of the distributions, such as the spreading along $p_{1||} = -p_{2||}$ due to the spatial extent of $\varphi^{(2)}(\mathbf{r}_2)$, depicted in panels (a,b) and (c,d), or the enhancement of the yields for unequal parallel momenta, which are the footprint of the Coulomb interaction (cf. lower panels), are present and can be seen. These features repeat themselves in the corresponding quantum mechanical calculations, presented in figure 3. Since both the classical and the quantum calculation incorporate the same form factor, this does not come as a surprise. The quantum distributions are, however, substantially broader, even though the underlying intensity of 3.0×10^{14} Wcm^{-2} is still far above the threshold intensity of 2.2×10^{14} Wcm^{-2}.

This picture changes below the threshold. In this region, electron-impact ionisation is classically forbidden throughout. The quantum calculation of figure 4 shows that the different interactions V_{12} and initial states have virtually no effect anymore on the momentum distribution, in marked contrast to the case for high intensities (see reference [16]). The maxima of the distribution occur at $p_{1||} = p_{2||} = \pm 2\sqrt{U_p}$ for the localized initial state and very slightly below this value for the $1s$ and $2p$ initial state. This implies that the electron returns near a zero of the electric field, even though its return energy would be somewhat higher at other times. The imaginary part $|\mathrm{Im}[t]|$ of the return time

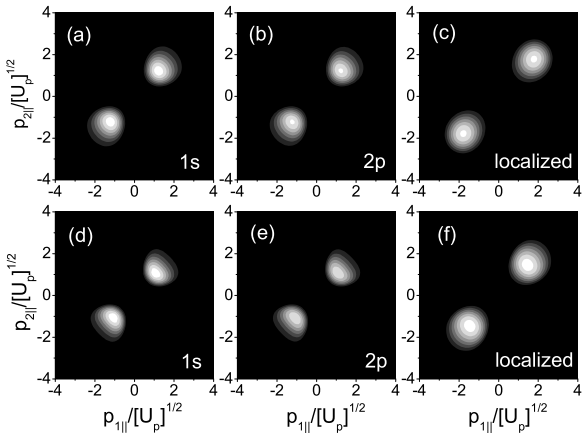

Figure 5. Same as figure 4, but computed using the classical model (11) with the second ionisation potential lowered according to equation (23).

is inversely related to the probability that the second electron be released. Indeed, it has a minimum near $p_{1||} = p_{2||} = \pm 2\sqrt{U_p}$ [32].

Classical models have also been used in the intensity range below the threshold [24]. This has been based on the fact that the second ionisation potential is actually lowered by the external driving field. For the singly charged ion, the second electron can escape over the saddle formed by its Coulomb potential and the potential of the driving field on one or the other side of the ion if its energy exceeds

$$E_{02}(t) = |E_{02}| - 2\sqrt{2|E(t)|}, \tag{23}$$

rather than $|E_{02}|$ if the lowering is ignored. Here $E(t) = 2\omega\sqrt{U_p}\sin\omega t$ is the instantaneous electric field at the time the first electron returns. This approximation has been successful in reducing the discrepancy in the probability for double ionisation between recollision calculations and experiment [24]. Very recently, differential measurements of nonsequential double ionisation have been performed at light intensities below the threshold [25], where electron impact ionisation is expected to be energetically forbidden. Nevertheless, the electron-electron momentum distribution just kept its shape when the laser intensity was reduced below this threshold. No qualitative evidence of the transition was observed. As a qualitative explanation, the afore-mentioned field-induced lowering of the second ionisation potential was proposed.

Classically, this time dependence can be incorporated in the δ function in equation (11) by replacing $|E_{02}|$ by $E_{02}(t)$. The results of such a calculation are shown in figure 5, which one might compare with the quantum-mechanical

calculation in figure 4 without a lowered threshold. Since the first electron now returns at times when the field is significantly different from zero, the two final-state electrons collect less energy from the field. This is reflected in the distributions in all cases considered, most strongly when the two electrons interact via the Coulomb potential. Moreover, the classical distributions are wider than their quantum-mechanical counter parts, since with the lowered threshold NSDI is classically allowed over a substantial range of return times. Unfortunately, there are no experimental data available for a comparison. The existing below-threshold data are for argon, where the contribution of a second mechanism, namely recollision-induced excitation of the second electron followed by tunneling [33], complicates the analysis.

6 Conclusions

The quantum-mechanical S-matrix element for nonsequential double ionisation via the rescattering scenario has been further investigated with regard to the effect of (i) the initial wave function of the second electron and (ii) the specific form of the interaction between the two electrons as expressed in the form factor. In particular, we have explored laser intensities around the threshold where the kinetic energy of the returning first-ionised electron just suffices to kick out the bound electron. We have compared the fully quantum-mechanical S matrix with a certain classical limit, which is known to produce virtually identical momentum distributions for intensities high above this threshold. For an intensity about 30% above the threshold, the classical limit already underestimates the width of the momentum distributions. Below the threshold, the classical model is no longer applicable. If, however, the fact is taken into account that the escape energy of the second electron is lowered in a time-dependent fashion by the presence of the laser field, the classical model can be reconsidered. The corresponding momentum distributions have been computed for this situation. For the case where the form factor is independent on the momenta, the classical model yields very compact expressions for the distributions of the momenta such that nonobserved components have been integrated over. This is applied to the one-electron energy spectrum in coincidence with nonsequential double ionisation. Good agreement with the available experimental data was found.

References

[1] R. Dörner, Th. Weber, M. Weckenbrock, A. Staudte, M. Hattas, H. Schmidt-Böcking, R. Moshammer, and J. Ullrich, Adv. At. Mol. Opt. Phys. **48** 1 (2002).
[2] Th. Weber, M. Weckenbrock, A. Staudte, M. Hattas, L. Spielberger, O. Jagutzki, V. Mergel, H.

Schmidt-Böcking, G. Urbasch, H. Giessen, H. Bräuning, C.L. Cocke, M.H. Prior, and R. Dörner, Opt. Express **8** 368 (2001).
[3] P.J. Ho, R. Panfili, S.L. Haan, and J.H. Eberly, Phys. Rev. Lett. **94** 093002 (2005).
[4] H.W. van der Hart, J. Phys. B **33** L699 (2000).
[5] G.L. Yudin and M.Yu. Ivanov, Phys. Rev. A **63** 033404 (2001).
[6] J. Chen, J. Liu, L.B. Fu and W.M. Zheng, Phys. Rev. A **63** 011404(R)(2001).
[7] L.B. Fu, J. Liu, J. Chen and S.G.Chen, Phys. Rev. A **63** 043416 (2001); J. Chen, J. Liu and W.M. Zheng, Phys. Rev. A **66** 043410 (2002).
[8] L.B. Fu, J. Liu, S.G. Chen, Phys. Rev. A **65** 021406(R)(2002).
[9] C. Figueira de Morisson Faria, X. Liu, W. Becker and H. Schomerus, Phys. Rev. A **69** 012402(R)(2004).
[10] C. Figueira de Morisson Faria, H. Schomerus, X. Liu and W. Becker, Phys. Rev. A **69** 043405 (2004).
[11] K. Sacha and B. Eckhardt, Phys. Rev. A **63** 043414 (2001); ibid. **64** 053401 (2001).
[12] B. Feuerstein, R. Moshammer and J. Ullrich, J. Phys. B **33** L8231 (2000).
[13] S.L. Haan, P.S. Wheeler, R. Panfili and J.H. Eberly, Phys. Rev. A **66** 061402(R)(2002); R. Panfili, S.L. Haan, and J.H. Eberly, Phys. Rev. Lett. **89** 113001 (2002).
[14] X. Liu and C. Figueira de Morisson Faria, Phys. Rev. Lett. **92** 133006 (2004).
[15] C. Figueira de Morisson Faria, X. Liu, A. Sanpera and M. Lewenstein, Phys. Rev. A **70** 043406 (2004).
[16] C. Figueira de Morisson Faria, A. Sanpera and M. Lewenstein, physics/0411096.
[17] A. Becker and F.H.M. Faisal, Phys. Rev. Lett. **84** 3546 (2000); ibid. **89** 193003 (2002); R. Kopold, W. Becker, H. Rottke, and W. Sandner, Phys. Rev. Lett. **85** 3781 (2000); S.V. Popruzhenko and S.P. Goreslavskii, J. Phys. B **34** L239 (2001); S.P. Goreslavskii and S. V. Popruzhenko, Opt. Express **8** 395 (2001).
[18] S.P. Goreslavskii, S.V. Popruzhenko, R. Kopold, and W. Becker, Phys. Rev. A **64**, 053402 (2001); S.V. Popruzhenko, Ph. A. Korneev, S.P. Goreslavskii and W. Becker, Phys. Rev. Lett. **89** 023001 (2002).
[19] B. Witzel, N.A. Papadogiannis, and D. Charalambidis, Phys. Rev. Lett. **85** 2268 (2000).
[20] E.R. Peterson and P.H. Bucksbaum, Phys. Rev. A **64** 053405 (2001).
[21] R. Lafon, J.L. Chaloupka, B. Sheehy, P.M. Paul, P. Agostini, K.C. Kulander, and L.F. DiMauro, Phys. Rev. Lett. **86** 2762 (2001).
[22] J.L. Chaloupka, R. Lafon, L.F. DiMauro, P. Agostini, and K.C. Kulander, Opt. Express **8** 352 (2001).
[23] J.L. Chaloupka, J. Rudati, R. Lafon, P. Agostini, K.C. Kulander, and L.F. DiMauro, Phys. Rev. Lett. **90** 033002 (2003).
[24] H.W. van der Hart and K. Burnett, Phys. Rev. A **62** 013407 (2000).
[25] E. Eremina, X. Liu, H. Rottke, W. Sandner, A. Dreischuh, F. Lindner, F. Grasbon, G.G. Paulus, H. Walther, R. Moshammer, B. Feuerstein, and J. Ullrich, J. Phys. B **36** 3269 (2003).
[26] C. Figueira de Morisson Faria, H. Schomerus, and W. Becker, Phys. Rev. A **66** 043413 (2002).
[27] L.D. Landau and E.M. Lifshitz, *Quantum Mechanics* (Pergamon Press, 1977)
[28] I.S. Gradsteyn and I.M. Ryzhik, *Table of Integrals, Series, and Products* (Academic Press, New York, 1980).
[29] R. Moshammer, J. Ullrich, B. Feuerstein, D. Fischer, A. Dorn, C.D. Schröter, J.R. Crespo L'opez-Urrutia, C. Höhr, H. Rottke, C. Trump. M. Wittmann, G. Korn, and W. Sandner, J. Phys. B **36** L113 (2003).
[30] D. B. Milosevic, and W. Becker, Phys. Rev. A **68** 065401 (2003).
[31] A. Becker, F.H.M. Faisal, Phys. Rev. Lett. **89** 193003 (2002).
[32] C. Figueira de Morisson Faria and W. Becker, Laser Phys. **13** 1196 (2003).
[33] V.L.B. de Jesus, B. Feuerstein, K. Zrost, D. Fischer, A. Rudenko, F. Afaneh, C.D. Schröter, R. Moshammer, and J. Ullrich, J. Phys. B **37** L161 (2004).